





# Low-loss plasmon-assisted electro-optic modulator

## Journal Article

### Author(s):

Haffner, Christian; [Chelladurai, Daniel](#) ; Fedoryshyn, Yuriy; [Josten, Arne](#) ; [Bäuerle, Benedikt](#) ; Heni, Wolfgang; Watanabe, Tatsuhiko; Cui, Tong; Cheng, Bojun; Saha, Soham; Elder, Delwin L.; Dalton, Larry R.; Boltasseva, Alexandra; Shalaev, Vladimir M.; Kinsey, Nathaniel; [Leuthold, Juerg](#) 

### Publication date:

2018

### Permanent link:

<https://doi.org/10.3929/ethz-b-000260913>

### Rights / license:

[In Copyright - Non-Commercial Use Permitted](#)

### Originally published in:

Nature 556, <https://doi.org/10.1038/s41586-018-0031-4>

# 1 **Low-loss plasmon-assisted electro-optic modulator**

2 **Christian Haffner<sup>1</sup>, Daniel Chelladurai<sup>1</sup>, Yuriy Fedoryshyn<sup>1</sup>, Arne Josten<sup>1</sup>, Benedikt Baeuerle<sup>1</sup>,**

3 **Wolfgang Heni<sup>1</sup>, Tatsuhiko Watanabe<sup>1</sup>, Tong Cui<sup>1</sup>, Bojun Cheng<sup>1</sup>, Soham Saha<sup>3</sup>, Delwin L. Elder<sup>2</sup>,**

4 **Larry. R. Dalton<sup>2</sup>, Alexandra Boltasseva<sup>3</sup>, Vladimir Shalaev<sup>3</sup>, Nathaniel Kinsey<sup>4</sup>, and Juerg Leuthold<sup>1</sup>**

5 *<sup>1</sup>ETH Zurich, Institute of Electromagnetic Fields (IEF), 8092 Zurich, Switzerland*

6 *<sup>2</sup>University of Washington, Department of Chemistry, Seattle, WA 98195-1700, USA*

7 *<sup>3</sup>Purdue University, School of Electrical & Computer Engineering and Brick Nanotechnology Center, West Lafayette, WIN 47909,*

8 *USA*

9 *<sup>4</sup>Virginia Commonwealth University, Department of Electrical and Computer Engineering, Richmond, VA 23284, USA*

10 **For nearly two decades, the field of plasmonics<sup>1</sup> - which studies the coupling of**  
11 **electromagnetic waves to the motion of free electrons in a metal<sup>2</sup> - has sought to realize**  
12 **subwavelength optical devices for information technology<sup>3-7</sup>, sensing<sup>8,9</sup>, nonlinear**  
13 **optics<sup>10,11</sup>, optical nanotweezers<sup>12</sup> and biomedical applications<sup>13</sup>. Although the heat**  
14 **generated by ohmic losses is desired for some applications (e.g. photo-thermal therapy),**  
15 **plasmonic devices for sensing and information technology have largely suffered from**  
16 **these losses<sup>14</sup>. This has led to a widespread stereotype that plasmonics is simply too lossy**  
17 **to be practical. Here, we demonstrate that these losses can be bypassed by employing**  
18 **“resonant switching”. In the proposed approach, light is only coupled to the lossy surface**  
19 **plasmon polaritons in the device’s off-state (in resonance) where attenuation is desired to**  
20 **ensure large extinction ratios and facilitate sub-ps switching. In the on-state (out of**  
21 **resonance), light is prevented from coupling to the lossy plasmonic section by destructive**  
22 **interference. To validate the approach, we fabricated a plasmonic electro-optic ring**  
23 **modulator. The experiments confirm that low on-chip optical losses (2.5 dB), high-speed**  
24 **operation ( $\gg 100$  GHz), good energy efficiency (12 fJ/bit), low thermal drift (4‰ K<sup>-1</sup>),**  
25 **and a compact footprint (sub- $\lambda$  radius of 1  $\mu$ m) can be realized within a single device.**

26 **Our result illustrates the potential of plasmonics to render fast and compact on-chip**  
27 **sensing and communications technologies.**

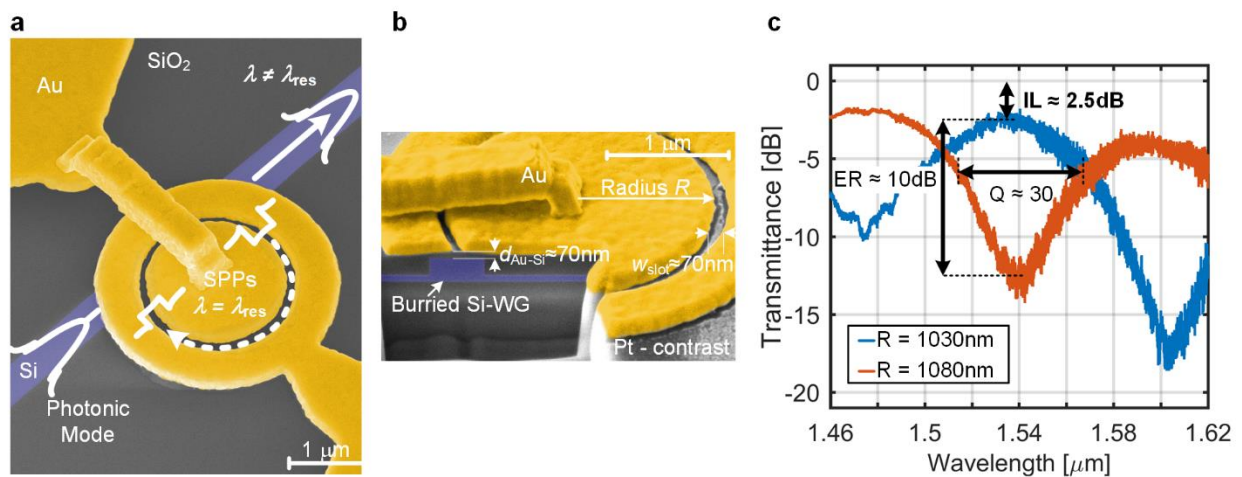
28

29 Telecommunication devices, such as electro-optic (EO) modulators must feature low  
30 insertion loss (IL) while providing a large phase ( $\Delta n$ ) or amplitude ( $\Delta\alpha$ ) change accumulated  
31 over a short device length<sup>15</sup>. Beyond that, modulators should offer low driving voltages and  
32 high-speed operation.

33 In recent years, silicon photonic active devices have emerged which benefit from low  
34 propagation losses (3 dB/mm) but have struggled to achieve large modulation depth for sub-  
35 mm devices ( $\Delta n$  and  $\Delta\alpha$ )<sup>16</sup>. State-of-the-art devices maximize their modulation through the use  
36 of resonant structures<sup>17</sup>, enabling compact ( $\mu\text{m}^2$ -sized) and energy efficient components<sup>18,19</sup>.  
37 However, the large Q-factor (on the order of a several 1000) limits the speed and increases the  
38 sensitivity of devices to temperature and fabrication fluctuations<sup>20</sup>. More recently, surface  
39 plasmonic polariton (SPP) devices have exploited the extreme confinement of light to achieve  
40 exceptional modulation within a few  $\mu\text{m}$  ( $\Delta n$  and  $\Delta\alpha$ )<sup>3,21</sup>. However, the metals that bring such  
41 promise to plasmonics are also the largest hindrance, as such devices suffer from large on-state  
42 loss ( $\sim\text{dB}/\mu\text{m}$ ). To combat plasmonic losses, some devices employ hybrid-plasmonic-photonic  
43 modes<sup>4,7,22</sup> while others minimize the length of the active section<sup>6,23</sup>. Still, typical IL of 10 dB  
44 due to the plasmonic propagation loss and photonic-to-plasmonic mode conversion loss remain  
45 a concern for high-speed state-of-the-art devices<sup>6,7</sup>. Thus, plasmonic on-chip technologies have  
46 been unable to replace the existing photonic or electronic solutions, placing the field of  
47 plasmonics at a crossroad to either abandon development or explore additional solutions.

48 We propose a novel approach, in which losses in plasmonic waveguides can be selectively  
49 used or bypassed to achieve low IL, strong modulation and high speed, simultaneously. This  
50 approach relaxes the prior goal to reduce the ohmic loss as much as possible to minimize the

51 device's on-state loss. Instead, we show that plasmonic losses can be harnessed by designing  
 52 the device geometry such that light passes through the lossy section when required (in the off-  
 53 state). To achieve this, we utilize a plasmonic ring resonator coupled to a buried low-loss  
 54 silicon photonic waveguide, see Fig. 1. Unlike prior approaches, which aim to reduce the  
 55 resonator loss to realize high  $Q$  cavities or lasing<sup>8,24-27</sup>, our resonator exhibits typical  
 56 propagation losses within the plasmonic cavity and mostly bypasses this lossy section in the  
 57 on-state through destructive interference. Using this design, we demonstrate for the first time,  
 58 a plasmonic modulator that is able to meet the key performance metrics of modern optical  
 59 communications links.



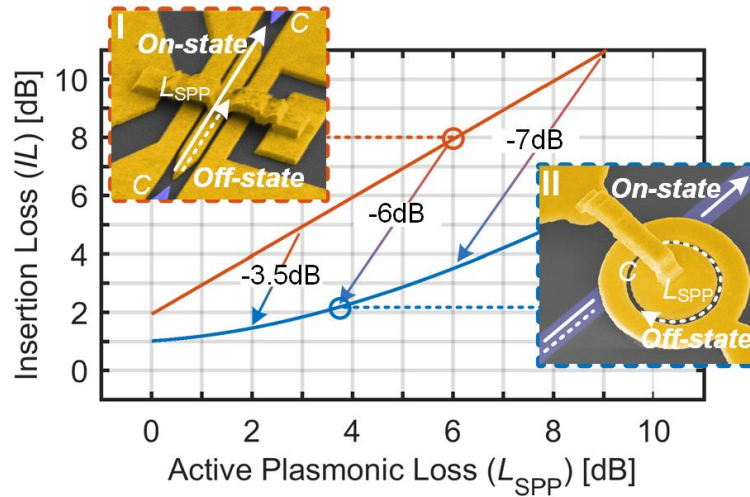
60  
 61 **Fig. 1:** False-colored SEM image of a plasmonic ring resonator and the corresponding transmittance over wavelength. (a) Top  
 62 view and (b) cross section of the resonator. Photonic modes propagating in the buried silicon waveguide resonator couple  
 63 partially to the SPPs in the metal-insulator-metal-ring when the resonance condition is fulfilled. While out of resonance  
 64 operation results in a low loss light transmission. (c) Passive measurements of two identical ring resonators that only differ in  
 65 radii (blue - 1030 nm; red - 1080 nm). Due to the resonant approach, insertion losses of 2.5 dB are measured with extinction  
 66 ratios (ER) above 10 dB.

67 Fig. 1 shows the proposed device geometry, which comprises a gold metal-insulator-metal  
 68 (MIM) slot waveguide ring coupled to a buried silicon bus waveguide, forming a notch filter  
 69 with a resonant wavelength of ( $\lambda_{res}$ ) (supplementary information: chapter II). The slot  
 70 waveguide is filled with an organic electro-optic (OEO) material which alters the device's

71 resonance condition through the Pockel's effect ( $\Delta n_{\text{SPP}}$ )<sup>28,29</sup>. This enables a fast and selective  
72 use of the plasmonic loss to attenuate the signal ( $\Delta\alpha$ ) in the bus waveguide by applying a  
73 voltage.

74 Fig. 1(c) shows the measured transmittance over the wavelength of two representative  
75 devices that differ in radius. For these structures, we have observed a distinct off-resonance  
76 ( $\lambda_0 \neq \lambda_{\text{res}}$ ) and on-resonance ( $\lambda_0 = \lambda_{\text{res}}$ ) condition at the telecommunication wavelength of  
77 1.54  $\mu\text{m}$  with an IL of 2.5 dB, an extinction ratio (ER) of 10 dB, and a Q-factor of  $\sim 30$ .  
78 Alternatively, we note that non-resonant devices based on MIM waveguides with a similar  
79 length feature an IL ranging from 8-10 dB<sup>6,7,23</sup>.

80 The reduced IL can be understood by comparing the exemplary operating principles of a  
81 non-resonant Mach-Zehnder (MZ)<sup>6</sup>, Fig. 2(I) and a resonant ring, Fig. 2(II). The IL of the  
82 device is a function of its coupling efficiency, geometry and accumulated ohmic loss. In both  
83 concepts, light couples to and from the plasmonic structure with a coupling efficiency ( $C$ ). A  
84 transmission modulation is then induced by the Pockels effect over an active plasmonic section  
85 of length or circumference ( $l$ ). The modulation depth ( $\Delta T$ ) – and also the loss ( $L_{\text{SPP}}$ ) – scale  
86 with the length of the active plasmonic section<sup>6</sup>. Fig. 2 shows the overall IL over the  $L_{\text{SPP}}$  in  
87 the active plasmonic area for a MZ and a critically coupled resonator. The arrows indicate the  
88 performance of devices with an equal  $\Delta T$ .

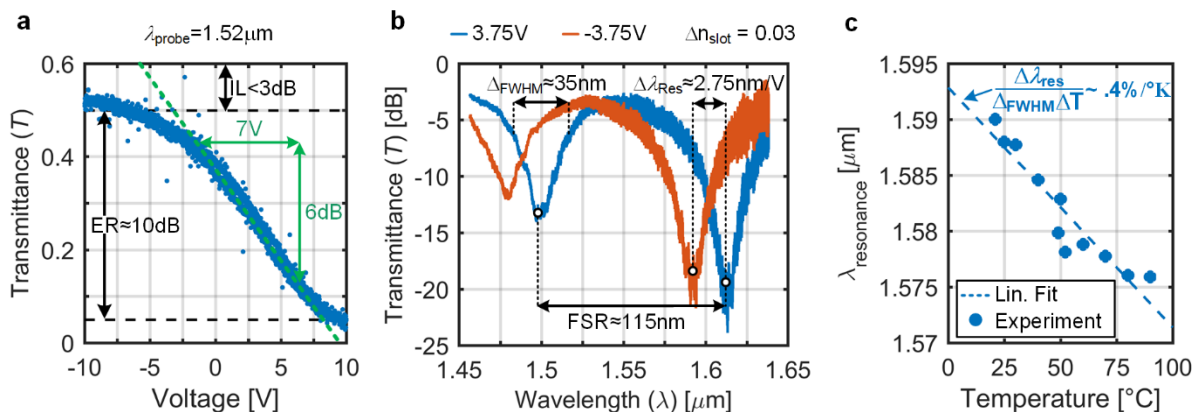


89

90 **Fig. 2:** Theoretical loss advantage of critical coupled resonator over non-resonant push-pull Mach-Zehnder devices. The IL are  
 91 plotted over the active plasmonic loss ( $L_{SPP}$ ) in the slot waveguide of the MZ (left inset, red) and resonator (right inset, blue).  
 92 Losses can be reduced by more than 6 dB. This is due to following reasons: I) bypassing mechanism – only a fraction of light  
 93 experiences plasmonic losses; II) resonant enhancement – resonators achieve the same phase shift for shorter devices (indicated  
 94 by the arrows); and III) coupling scheme – non-resonant approaches require two photonic/SPP converters while resonant  
 95 approaches require only one.

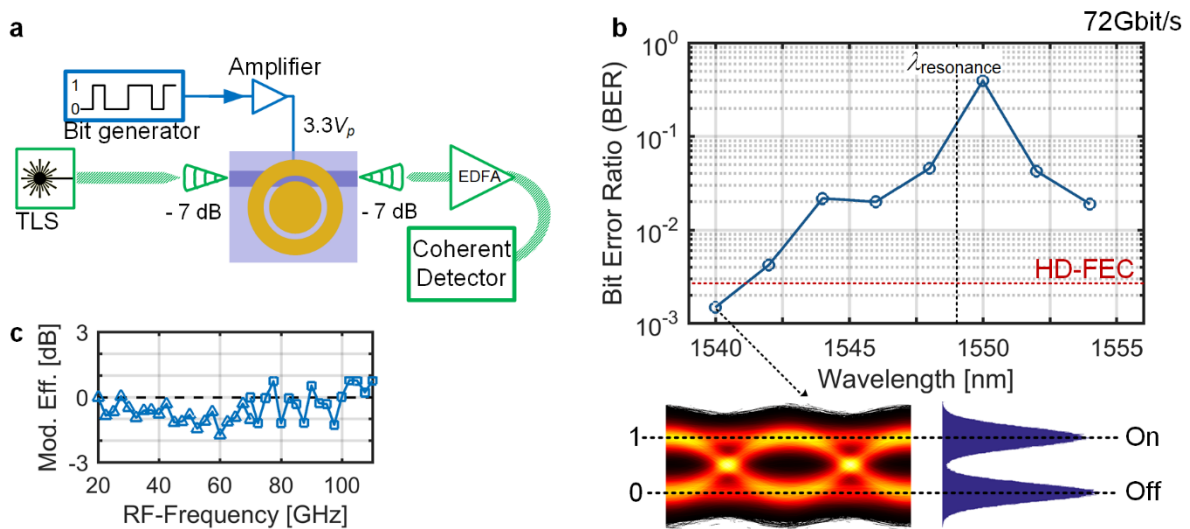
96 The following points arise from Fig. 2. First, the resonator's loss is always smaller (blue curve  
 97 < red curve) due to the bypassing mechanism<sup>30</sup>. Second, the resonator has a 1 dB lower IL at  
 98  $L_{SPP} \approx 0$  dB. This is because the non-resonant device requires two photonic-SPP converters as  
 99 both the on- and the off-state propagate through the plasmonic section. Ohmic losses in the  
 100 converters limit the conversion efficiency ( $C$ ) to  $\sim 1$  dB<sup>23,31</sup>. Contrarily, the selection  
 101 mechanism of the resonator (on-state  $\rightarrow$  bus waveguide; off-state  $\rightarrow$  ring) requires a converter  
 102 which couples only a fraction of the light to the ring. Third, in the ring we take advantage of  
 103 the resonantly enhanced  $\Delta T$  to reduce the device length (supplementary information: chapter  
 104 VII). For our resonant structures, we have calculated an enhancement of  $\sim 1.5$ . Consequently,  
 105 our ring with a circumference of  $l = 6 \mu\text{m}$  ( $L_{SPP} \approx 4$  dB) offers the same transmittance change  
 106 as a MZ of  $l = 9 \mu\text{m}$  ( $L_{SPP} \approx 6$  dB). In total, the ring device offers a 6 dB IL advantage over the  
 107 MZ modulator. Additionally, losses can be further reduced by under-coupling the resonator as  
 108 limited ERs of 10 dB are sufficient for many practical applications<sup>32</sup>.

109 To illustrate the modulation performance ( $\Delta T$ ) of the plasmonic resonator, the SPPs' effective refractive index ( $\Delta n_{\text{SPP}}$ ) is altered by applying a bias between the inner and outer rings<sup>28</sup>. Fig. 3(a) shows the transmitted power versus applied voltage for a wavelength of 110  $\sim 1.52 \mu\text{m}$ . We observed an IL  $< 3 \text{ dB}$ , an ER of  $\sim 10 \text{ dB}$ , and a linear response (dashed green line) for a peak voltage of 3.5 V with an ER of  $\sim 6 \text{ dB}$ . This performance in terms of IL and ER 111 is similar to well-developed CMOS photonic resonators<sup>20</sup>. We estimate that operation under a digital driving voltage ( $1 \text{ V}_{\text{pp}}$ )<sup>20</sup> is achievable in the near future by utilizing other plasmonic 112 materials like silver or copper, using the newest OEO-materials and improving fabrication 113 (supplementary information: chapter VIII). To highlight the mechanism of the modulation the transmission of the device has been measured under a positive and negative bias of  $\pm 3.75 \text{ V}$  as 114 a function of wavelength, see Fig. 3(b). This results in a normalized sensitivity ( $S_{\lambda}/\Delta_{\text{FWHM}} = \Delta\lambda_{\text{res}}/(\Delta_{\text{FWHM}} \cdot \Delta n)$ ) of  $\sim 17 \text{ RIU}^{-1}$ , assuming a relative change in OEO's refractive index of 115  $\sim 0.03$ . This can be compared to commercial SPR sensors that achieve values of  $50 \text{ RIU}^{-1}$  using 116 a free-space Kretschmann configuration<sup>33</sup>. So, currently our approach is already close to the 117 non-integrated free space approaches.



124 **Fig. 3** Sensitivity and stability of the plasmonic resonator. (a) Voltage sensitivity of the resonator's transmittance. (b) 125 Sensitivity of the ring as a function of the wavelength. A small change ( $\Delta n_{\text{slot}} \approx 0.03$ ) in the refractive index of the slot-filling 126 material causes a large change of the resonance wavelength (blue/red). (c) The resonator shows stable operation across a large 127 thermal variation. These characteristics make the plasmonic MIM-ring resonator a promising candidate in the field of optical 128 modulators and sensors. 129

130 The moderate Q-factor guarantees a high operational speed and provides good thermal  
 131 stability. For example, the measured resonance frequency is plotted in Fig. 3(c) over a  
 132 temperature range from 20°C up to 90°C. In this case, the resonant frequency is found to follow  
 133 a linear trend line with a slope of  $\sim 0.4\% \text{ K}^{-1}$ . The insensitivity of the plasmonic resonator to  
 134 temperature fluctuations is in strong contrast to photonic resonators, which are two orders of  
 135 magnitude more sensitive to temperature fluctuations ( $\sim 100\% \text{ K}^{-1}$ )<sup>19</sup>. This is extremely  
 136 beneficial for applications where strong temperature fluctuations occur. For example, a  
 137 plasmonic resonant sensor or modulator would be immune to thermal fluctuations of  $\pm 5 \text{ }^\circ\text{C}$   
 138 which normally occur in CPUs while photonic resonators require power-consuming  
 139 temperature controls to maintain operation<sup>20</sup>. Furthermore, the moderate Q factors are also  
 140 beneficial for high-speed operation as desired in electro-optic modulators. As a result, we are  
 141 able to push the bandwidth of a resonant electro-optic modulator well beyond 100 GHz  
 142 (supplementary information: chapter XIII). In comparison, photonic resonators are more likely  
 143 limited to bandwidths of  $\sim 20 \text{ GHz}$  and below<sup>19,20</sup>.



144  
 145 **Fig. 4:** High-speed data experiments with a plasmonic ring resonator used as an EO-modulator. (a) Depicts the experimental  
 146 setup. (b) Bit-error-ratio (BER) vs. wavelength for a resonator with  $\lambda_{\text{resonance}} = 1549 \text{ nm}$ . BERs below the hard-decision forward  
 147 error correction (HD-FEC) limit show successful data modulation and detection without the use of a temperature control. The  
 148 BER increases at the resonance wavelength as expected from the notch-filter response of the resonator. (c) Shows the  
 149 bandwidth of the plasmonic resonator in the bottom, which is beyond 110 GHz.



150 Subsequently, we performed high-speed data experiments to demonstrate the robustness, high  
151 speed and low power switching capability. Although, the “resonant switching” principle can  
152 also be used to optimize sensors, we focus on high speed applications because their sensitivity  
153 and stability requirements are stricter.

154 In the experiment of Fig. 4(a) the peak driving voltage was  $\sim 3.3 V_{\text{peak}}$  and the laser  
155 wavelength was varied to capture the response of the modulator. Low device losses of 2.5 dB  
156 and fiber-to-silicon waveguide losses of  $\sim 7$  dB resulted in fiber-to-fiber coupling losses of 16.5  
157 dB enabling successful operation with low laser powers of 4 dBm and below. The resulting bit-  
158 error-ratio (BER) versus wavelength for a 72 Gbit/s signal is shown in Fig. 4(b) where a peak  
159 in the BER is observed at  $\lambda_{\text{res}}$ . A high BER is observed at  $\lambda_{\text{res}}$  since applying the same voltage  
160 with an opposing sign results in the same optical amplitude but a different phase. Consequently,  
161 we confirmed that the operating mechanism relies on amplitude modulation. Off-resonance,  
162 the BER quickly dropped to  $\sim 1 \times 10^{-3}$  which is below the hard-decision forward error correction  
163 (HD-FEC) limit and allows for successful data modulation and detection<sup>34</sup>. No thermal heater  
164 was required for stabilization. Additionally, we reduced the data-rate to 36 Gbit/s and 18 Gbit/s  
165 and found BERs of  $\sim 2 \times 10^{-6}$  and  $< 1 \times 10^{-6}$ , respectively, indicating that the BER at 72 Gbit/s is  
166 mainly limited by the electrical equipment (supplementary information: chapter XIV). We  
167 estimate the energy consumption of the modulator to be  $\sim 12$  fJ/bit at 72 Gbit/s<sup>15</sup> for a device  
168 capacitance of 1.1 fF.

169

170 We demonstrate that low-Q resonant designs can enable low-loss active plasmonic devices  
171 with a good modulation depth by utilizing highly confined SPPs. We believe that our approach  
172 – unlike conventional resonant photonics – breaks the trade-off between sensitivity (high-Q)  
173 on the one hand and speed and temperature stability (low-Q) on the other. Our work can be  
174 seen as a step towards practical plasmonics that ultimately serves as a compact and fast gateway

175 between electronics (local signal processing) and photonics (broad bandwidth and low-loss  
176 data stream). The proposed slot waveguide approach could also open many applications in  
177 sensing because the resonant response can be exploited for many other material systems  
178 ranging from low index materials like aqueous solutions to high index materials such as silicon.  
179

180 **Supplementary information and methods are given in the supplementary**  
181 **information manuscript.** The datasets generated during and/or analysed during the current  
182 study are available from the corresponding author on reasonable request.  
183

#### 184 **References:**

- 185 1 Maier, S. A. *et al.* Plasmonics—A Route to Nanoscale Optical Devices. *Advanced Materials* **13**, 1501-  
186 1505 (2001).
- 187 2 Gramotnev, D. K. & Bozhevolnyi, S. I. Plasmonics beyond the diffraction limit. *Nat Photonics* **4**, 83-91,  
188 doi:10.1038/nphoton.2009.282 (2010).
- 189 3 Dionne, J. A., Diest, K., Sweatlock, L. A. & Atwater, H. A. PlasMOSStor: A Metal–Oxide–Si Field Effect  
190 Plasmonic Modulator. *Nano Letters* **9**, 897-902, doi:10.1021/nl803868k (2009).
- 191 4 Sorger, V. J., Lanzillotti-Kimura Norberto, D., Ma, R.-M. & Zhang, X. Ultra-compact silicon  
192 nanophotonic modulator with broadband response. *Nanophotonics* **1**, 17, doi:10.1515/nanoph-2012-  
193 0009 (2012).
- 194 5 Melikyan, A. *et al.* High-speed plasmonic phase modulators. *Nat Photon* **8**, 229-233 (2014).
- 195 6 Haffner, C. *et al.* All-plasmonic Mach–Zehnder modulator enabling optical high-speed communication  
196 at the microscale. *Nat Photon* **9**, 525-528 (2015).
- 197 7 Keeler, G. A. *et al.* in *Optical Fiber Communication Conference*. Th3I.1 (Optical Society of America),  
198 (2017).
- 199 8 Min, B. *et al.* High-Q surface-plasmon-polariton whispering-gallery microcavity. *Nature* **457**, 455-458  
200 (2009).
- 201 9 Brolo, A. G. Plasmonics for future biosensors. *Nat Photon* **6**, 709-713 (2012).
- 202 10 Cai, W., Vasudev, A. P. & Brongersma, M. L. Electrically Controlled Nonlinear Generation of Light  
203 with Plasmonics. *Science* **333**, 1720-1723, doi:10.1126/science.1207858 (2011).
- 204 11 Kauranen, M. & Zayats, A. V. Nonlinear plasmonics. *Nat Photon* **6**, 737-748 (2012).
- 205 12 Ndukaife, J. C. *et al.* Long-range and rapid transport of individual nano-objects by a hybrid  
206 electrothermoplasmonic nanotweezer. *Nat Nano* **11**, 53-59, doi:10.1038/nnano.2015.248 (2016).
- 207 13 Hirsch, L. R. *et al.* Nanoshell-mediated near-infrared thermal therapy of tumors under magnetic  
208 resonance guidance. *Proceedings of the National Academy of Sciences* **100**, 13549-13554,  
209 doi:10.1073/pnas.2232479100 (2003).
- 210 14 Khurgin, J. B. How to deal with the loss in plasmonics and metamaterials. *Nat Nano* **10**, 2-6,  
211 doi:10.1038/nnano.2014.310 (2015).
- 212 15 Miller, D. A. B. Attojoule Optoelectronics for Low-Energy Information Processing and  
213 Communications; a Tutorial Review. *J. Lightwave Technol.* **PP**, 1-1, doi:10.1109/JLT.2017.2647779  
214 (2017).
- 215 16 Reed, G. T., Mashanovich, G., Gardes, F. Y. & Thomson, D. J. Silicon optical modulators. *Nat Photon*  
216 **4**, 518-526 (2010).
- 217 17 Vahala, K. J. Optical microcavities. *Nature* **424**, 839-846 (2003).
- 218 18 Xu, Q., Schmidt, B., Pradhan, S. & Lipson, M. Micrometre-scale silicon electro-optic modulator. *Nature*  
219 **435**, 325-327 (2005).

- 220 19 Timurdogan, E. *et al.* An ultralow power athermal silicon modulator. *Nat Commun* **5**,  
221 doi:10.1038/ncomms5008 (2014).  
222 20 Sun, C. *et al.* Single-chip microprocessor that communicates directly using light. *Nature* **528**, 534-538,  
223 doi:10.1038/nature16454 (2015).  
224 21 Emboras, A. *et al.* Atomic Scale Plasmonic Switch. *Nano Letters*, doi:10.1021/acs.nanolett.5b04537  
225 (2015).  
226 22 Oulton, R. F., Sorger, V. J., Genov, D. A., Pile, D. F. P. & Zhang, X. A hybrid plasmonic waveguide for  
227 subwavelength confinement and long-range propagation. *Nat Photon* **2**, 496-500 (2008).  
228 23 Zhu, S., Lo, G. Q. & Kwong, D. L. Phase modulation in horizontal metal-insulator-silicon-insulator-  
229 metal plasmonic waveguides. *Opt. Express* **21**, 8320-8330, doi:10.1364/OE.21.008320 (2013).  
230 24 Hill, M. T. *et al.* Lasing in metallic-coated nanocavities. *Nat Photon* **1**, 589-594 (2007).  
231 25 Bozhevolnyi, S. I., Volkov, V. S., Devaux, E., Laluet, J.-Y. & Ebbesen, T. W. Channel plasmon  
232 subwavelength waveguide components including interferometers and ring resonators. *Nature* **440**, 508-  
233 511 (2006).  
234 26 Kress, S. J. P. *et al.* A customizable class of colloidal-quantum-dot spasers and plasmonic amplifiers.  
235 *Science Advances* **3**, doi:10.1126/sciadv.1700688 (2017).  
236 27 Zhu, W. *et al.* Surface plasmon polariton laser based on a metallic trench Fabry-Perot resonator. *Science*  
237 *Advances* **3**, doi:10.1126/sciadv.1700909 (2017).  
238 28 Sun, S. S. & Dalton, L. R. *Introduction to Organic Electronic and Optoelectronic Materials and Devices*.  
239 (Taylor & Francis, 2008).  
240 29 Elder, D. L. *et al.* Effect of Rigid Bridge-Protection Units, Quadrupolar Interactions, and Blending in  
241 Organic Electro-Optic Chromophores. *Chemistry of Materials*, doi:10.1021/acs.chemmater.7b02020  
242 (2017).  
243 30 Zanotto, S., Morichetti, F. & Melloni, A. Fundamental limits on the losses of phase and amplitude optical  
244 actuators. *Laser & Photonics Reviews* **9**, 666-673 (2015).  
245 31 Delacour, C. *et al.* Efficient Directional Coupling between Silicon and Copper Plasmonic Nanoslot  
246 Waveguides: toward Metal–Oxide–Silicon Nanophotonics. *Nano Letters* **10**, 2922-2926,  
247 doi:10.1021/nl101065q (2010).  
248 32 Bogaerts, W. *et al.* Silicon microring resonators. *Laser & Photonics Reviews* **6**, 47-73 (2012).  
249 33 Becker, J., Trügler, A., Jakab, A., Hohenester, U. & Sönnichsen, C. The Optimal Aspect Ratio of Gold  
250 Nanorods for Plasmonic Bio-sensing. *Plasmonics* **5**, 161-167, doi:10.1007/s11468-010-9130-2 (2010).  
251 34 Chang, F., Onohara, K. & Mizuochi, T. Forward error correction for 100 G transport networks. *IEEE*  
252 *Communications Magazine* **48** (2010).  
253

254 **Supplementary Information** is linked to the online version of the paper at  
255 [www.nature.com/nature](http://www.nature.com/nature).

256

257 **Acknowledgment:** The authors thank Ute Drechsler and Hans-Rudolf Benedickter for  
258 their technical assistance. Also we would like to acknowledge partial funding of this project by  
259 the EU Project PLASMOFAB (688166), by the ERC grant PLASILOR (640478), by the  
260 National Science Foundation (NSF) (DMR-1303080) and by the Air Force Office of Scientific  
261 Research grants (FA9550-15-1-0319 and FA9550-14-1-0138). N. K. acknowledges support  
262 from the Virginia Microelectronics Consortium and the Virginia Commonwealth University  
263 Presidential Research Quest Fund. This work was carried out at the BRNC Zurich and ETH  
264 Zurich.

265

266 **Author contributions:**

267 C.H., N.K., V.S., A.B. and J.L. conceived the concept and supervised the project. C.H.,  
268 D.C., S.S., and T.C. designed the modulator and developed the analytic frame work for fast  
269 optimization. T.W. designed the photonic grating coupler. C.H., D.C. and Y.F. fabricated the  
270 modulator and developed the required process technology. B.C. developed a focused ion beam  
271 process to image the cross section with minimal destructive influence on the suspended bridge.  
272 D.L.E., W.H., C.H., and L.R.D. developed, synthesized and implemented the poling procedure  
273 of the OEO-material for plasmonic ring resonators. C.H., and J.L., designed the experiments.  
274 C.H., D.C. and T.C. performed the passive characterization. C.H. performed the temperature  
275 sensitivity, DC switching and electro-optic bandwidth experiments. B.B., A.J. and C.H.  
276 performed the high-speed data experiment. B.B. and A.J. designed, calibrated, and automated  
277 the high-speed data experiment. B.B. and A.J. developed the digital-signal processing for data  
278 generation and analysis of the high-speed data experiment. All authors discussed and analysed  
279 the data. C.H., N.K., D.C., and J.L. wrote the manuscript.

280

281 **Author information:**

282 Reprints and permissions information is available at [www.nature.com/reprints](http://www.nature.com/reprints). No author has  
283 an competing financial interest. Correspondence and requests for materials should be addressed  
284 to [haffnerc@ethz.ch](mailto:haffnerc@ethz.ch).

285